

Aleksandra Rewolińska¹, Łukasz Wojciechowski², Krzysztof Kubiak³

Tribological Studies of Braided Packings with Natural and Expanded Graphite under Dry and Water-Lubricated Conditions

Badania tribologiczne pakunków plecionych z grafitem naturalnym i ekspandowanym w warunkach suchych i w środowisku wodnym

Key words: natural graphite, expanded graphite, coefficient of friction, wear, transfer layers, water-lubricated conditions

Abstract

The aim of this study was to evaluate the tribological properties of braided packings impregnated with natural graphite (NG) and expanded graphite (EG), operating against AISI 4130 alloy steel under dry and water-lubricated conditions. Tests were performed using an Amsler A135 tester in the “block–ring” configuration at a load of 350 N, speed of 200 rpm, and a duration of 30 minutes. The coefficient of friction, operating temperature, and mass wear were determined, and SEM/EDS analyses were carried out to characterize transfer layers. The results demonstrated a significant influence of graphite type and operating environment on friction behavior. Under dry conditions, EG-based packings exhibited a lower coefficient of friction (0.11 vs. 0.24 for NG), reduced operating temperature (by ~30%), and markedly lower mass wear. In water-lubricated conditions, COF values remained more favorable for EG; however, its mass wear increased by 367%, while for NG the increase was only 15%. SEM and EDS analyses revealed that expanded graphite formed more uniform and adhesive transfer layers under dry conditions, which promoted friction stabilization. In the presence of water, these films became less homogeneous. Natural graphite in the water-lubricated environment exhibited weak adhesion to the substrate and discontinuous coverage of the steel surface.

Słowa kluczowe: grafit naturalny, grafit ekspandowany, współczynnik tarcia (COF), zużycie, warstwy transferowe, środowisko wodne

Streszczenie

Celem pracy była ocena właściwości tribologicznych pakunków plecionych impregnowanych grafitem naturalnym (NG) i ekspandowanym (EG), współpracujących ze stalą stopową AISI 4130 w warunkach tarcia suchego i w środowisku wodnym. Badania przeprowadzono z użyciem testera Amsler A135 w układzie „blok–pierścieni” przy obciążeniu 350 N, prędkości 200 obr./min i czasie 30 min. Analizowano współczynnik tarcia (COF), temperaturę pracy oraz zużycie masowe próbek. Dodatkowo wykonano obserwacje SEM/EDS w celu oceny warstw transferowych. Wyniki wykazały istotny wpływ rodzaju grafitu i warunków pracy na procesy tarcia. W środowisku suchym pakunki z EG charakteryzowały się niższym COF (0,11 wobec 0,24 dla NG), obniżoną temperaturą pracy (ok. 30%) oraz znacząco mniejszym zużyciem masowym. W środowisku wodnym wartości COF pozostawały korzystniejsze dla EG, jednak jego zużycie masowe wzrosło o 367%, podczas gdy w przypadku NG wzrost wyniósł jedynie 15%. Analiza SEM i EDS wykazała, że grafit ekspandowany tworzy bardziej równomierne i adhezyjne warstwy transferowe w warunkach suchych, co sprzyja stabilizacji tarcia. W obecności wody warstwy te stawały się mniej jednorodne. Grafit naturalny w środowisku wodnym wykazywał słabą adhezję do podłoża i nieciągłe pokrycie powierzchni stali.

Introduction

Solid lubricants play a crucial role in reducing wear and stabilizing friction in tribological pairs operating under a wide range of loads, speeds, and environmental conditions [1–3]. Among the commonly used solid lubricants are carbon-based materials [4,5], such as natural graphite and expanded graphite. They are characterized by high thermal conductivity, layered structure, ability to dissipate heat generated during friction, and a relatively stable

¹ORCID: 0000-0002-6342-0761. Poznan University of Technology, Faculty of Civil and Transport Engineering, Institute of Machines and Motor Vehicles, Piotrowo 3a Street, 60-965 Poznan, Poland, aleksandra.rewolinska@put.poznan.pl

²ORCID: 0000-0003-3682-6368. Poznan University of Technology, Faculty of Civil and Transport Engineering, Institute of Machines and Motor Vehicles, Piotrowo 3a Street, 60-965 Poznan, Poland, lukasz.wojciechowski@put.poznan.pl

³ORCID: 0000-0002-6571-2530. University of Leeds, School of Mechanical Engineering, Faculty of Engineering and Physical Sciences, Leeds, LS2 9JT, United Kingdom, K.Kubiak@leeds.ac.uk

coefficient of friction (COF). Both materials are allotropic forms of the same element—carbon—but they differ significantly in terms of structure and physicochemical properties [6]. The available literature contains extensive data on the effect of natural graphite on the tribological properties of materials. Much less attention has been devoted to expanded graphite, indicating a research gap in this area. Comparative studies evaluating the performance of both graphite forms under different operating conditions are also scarce.

Hajdukiewicz et al. [7] analyzed the influence of natural graphite content on the tribological and structural properties of polyester–glass recyclate composites against a steel counter-sample. The results showed that the addition of graphite at 2%, 5%, and 10% significantly affected the wear behavior and mass wear rate of the composite. The best results were obtained with 10% graphite, which markedly reduced COF. Similar results were reported by Baptista et al. [8], who demonstrated that increasing graphite filler content in epoxy composites reduced fatigue-related wear. However, the effect of natural graphite addition is not always consistent. Alajmi et al. [9] found that higher graphite content (≥ 5 wt%) in epoxy composites significantly worsened their tribological performance. Kolluri et al. [10] studied the influence of natural graphite particle size in friction composites and showed that finer particles enabled more effective heat dissipation during braking. In a subsequent study, Kolluri et al. [11] compared phenolic composites filled with natural and synthetic graphite. Temperature was found to be a decisive factor for composite performance regardless of graphite type or particle size. Composites with synthetic graphite exhibited better friction resistance, while those with natural graphite showed the highest wear resistance. Aranganathan et al. [12] investigated friction materials containing thermographite (TG) and natural graphite (NG) and found that TG-based materials demonstrated superior properties in nearly all aspects compared with NG. Demi [13] reported that increasing graphite content in ARC-152 epoxy composites reduced wear volume by up to 96% (12 wt%) and 93% (4 wt%), accompanied by a decrease COF with higher graphite content and load. Microstructural analysis confirmed reduced abrasive wear, lower surface porosity, and shallower wear craters. Basavarajappa et al. [14,15] examined epoxy composites with 0%, 5%, and 10 wt% graphite and found that mass loss increased with sliding speed and load, but overall wear resistance improved with graphite addition due to the formation of a uniform lubricating film.

Research has also been conducted on expanded graphite (EG), which shows promising potential in reducing wear and stabilizing friction. Dinker et al. [16] investigated beeswax/EG composites for thermal energy storage, showing that the combination of thermal stability and lubricating properties makes EG a suitable candidate for tribological materials with enhanced wear resistance. Struchkova et al. [17] demonstrated that adding 15 wt% EG to PTFE reduced wear rate by up to 50% compared with PTFE filled with commercial graphite. Wang et al. [18] found that nitrile–butadiene rubber (NBR) nanocomposites with EG had superior wear resistance compared with their microcomposite counterparts. Jia et al. [19] studied polyimide (PI) composites reinforced with nanoscale EG and reported optimal friction reduction and wear resistance at 15 wt% EG. Jin et al. [20] compared the friction and wear behavior of NG and EG, showing that EG exhibited better tribological performance, maintaining COF in the range of 0.3–0.5, ensuring effective braking, and reducing wear rate by 22.43% compared with NG.

Overall, the use of graphite-based materials generally improves the tribological performance of frictional and sliding components, enhancing durability and efficiency, particularly under demanding operating conditions. However, limited data exist on the interaction of natural and expanded graphite with metallic materials. The mechanisms of formation and the role of lubricating films on contact surfaces remain insufficiently understood. In particular, the behavior of both graphite forms in the presence of water has not been adequately studied, even though many sources indicate the significant role of water in graphite-based tribological systems. The lubricating properties of graphite have been shown, both experimentally and through simulations [21,22], to depend strongly on humidity. This is due to graphite's ability to form strong chemical bonds with water molecules, as water vapor adsorbs at the crystallographic edges, weakening interlayer interactions and facilitating shearing and transfer onto mating surfaces [23]. While it is widely acknowledged that graphite promotes the

formation of a lubricating film, its exact role in lubrication remains unclear. For example, Jia et al. [24] and Hirani and Goilkar [25] observed that water may hinder film formation, whereas Restuccia et al. [26] reported that water reduced COF in graphite-containing tribological pairs. Burroto et al. [27] showed that surface wettability plays a critical role in friction and wear under water lubrication. SEM observations confirmed that water lubrication can enhance performance when hydrophilic and hydrophobic materials, such as carbon fibers, are paired. In particular, for hydrophobic discs against hydrophilic pins, both COF and wear were lower than under oil lubrication. Jia et al. [28] compared four polymer composites reinforced with carbon fibers tested against stainless steel under dry and water-lubricated conditions. All composites exhibited lower COF and higher wear resistance under water lubrication than under dry sliding. Moreover, water lubrication suppressed transfer film formation on the steel ring, reducing its effect on tribological behavior compared with dry conditions. In contrast, Lancaster [29,30] studied carbon-fiber-reinforced polymers under water, aqueous solutions, and organic fluids, reporting higher wear under water lubrication than under dry friction, attributed to the inability to form a transfer film.

In summary, the role of water in graphite-containing tribological pairs remains ambiguous. Water may significantly affect friction and wear mechanisms in specific technical applications. This represents a critical research gap requiring further investigation.

The objective of this study is to compare the tribological properties of braided packings containing natural and expanded graphite and to identify the mechanisms governing their behavior in contact with alloy steel under dry and water-lubricated conditions.

Materials and Research Methods

Tribological tests were carried out using an Amsler tester, model A135, in a block–ring configuration (Fig. 1). This device allows for both continuous and static adjustment of load, variation of the counter-sample's rotational speed, as well as temperature measurement using a thermocouple.

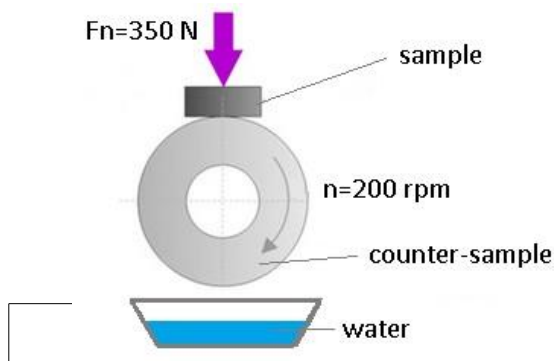


Figure 1. Diagram of the analyzed friction pair
Rysunek 1. Wykres analizowanego węzła tarcia

Commercially available braided packings (cords), commonly used in sealing technology, were selected for the tests. The samples were cut to dimensions of $10 \times 10 \times 15\text{ mm}$ (height \times width \times depth). The cords were made of synthetic PTFE fibers, impregnated with either natural graphite (NG) or expanded graphite (EG) through impregnation, ensuring uniform graphite distribution throughout the fiber structure and consistent tribological properties. The graphite content in the tested cords was approximately 50%. In the following sections of this work, the samples are referred to as “NG packing” (with natural graphite) and “EG packing” (with expanded graphite). The counter-sample was a ring made of AISI 4130 alloy steel, with an outer diameter of 45 mm and a width of 12 mm. The working surface of the rings was characterized by a roughness of $R_a \approx 0.5\text{ }\mu\text{m}$. The chemical composition of the graphite materials and alloy steel, as well as their physicochemical and mechanical properties, are presented in Tables 1 and 2, respectively.

Table 1. Chemical composition of graphite materials and alloy steel
Tabela 1. Skład chemiczny materiałów grafitowych oraz stali stopowej

Graphite material	Chemical composition
Expanded graphite (EG)	C-98, O-0,5-1, S-0,01-0,1, Si, Al, Fe, Ca, Mg-0,5-2
Natural graphite (NG)	C-95–99,5, Fe, Si, Al, Ca 0,5-5
Alloy steel (AISI 4130)	Fe-96, C-0,28-0,33, Cr-0,8-1,1, Mn-0,4-0,6, P-0,035, Si-0,15-0,35, S-0,035

Table 2. Physical and mechanical properties of expanded graphite, natural graphite, and AISI steel [based on 31,32,33]

Tabela 2. Właściwości fizyczne i mechaniczne grafitu ekspandowanego, naturalnego i stali AISI [opracowano na podstawie 31,32,33]

Properties	Expanded graphite	Natural graphite	Alloy steel (AISI 4130)
Density [kg/m ³]	1,600	2,260	
Roughness Ra [μm]	–	–	0.5
Hardness [HB]	–	–	218
Tensile strength [MPa]	0.1–1	10–25	560
Volumetric expansion [m ³ /s]	$(0.69–1.11) \times 10^{-7}$	$(0.28–1.39) \times 10^{-9}$	–
Specific surface area [x10 ³ m ² /kg]	40–200	3.5–20	0.01–0.1
Yield strength [MPa]	–	–	460
Thermal conductivity [W/mK]	25–470	120–400	42.7
Elasticity (Young's modulus) [x10 ³ MPa]	very low (<1)	10–20	205–210

To identify the tribological phenomena occurring in the analyzed material pairs, tests were carried out under dry and wet friction conditions. In the case of wet tests, the steel ring was partially immersed in water, which ensured a constant supply of the lubricating medium to the tribological contact area. The relative humidity in the testing room was 41%. The tests were performed under the following kinetic parameters: ring rotational speed – 200rpm, load – 350N, test duration – 30 minutes. The testing conditions are presented in Table 3.

Table 3. Operating conditions of the friction pair during the test

Tabela 3. Warunki pracy pary ciernej podczas badania

Conditions	Dry	Water
Relative humidity in the testing room [%]		41
Test duration [min]		30
Rotational speed [rpm]		200
Load [N]		350

The tribological behavior was analyzed based on the measured values of friction torque and the coefficient of friction (COF) calculated from it, as well as the operating temperature of the friction pair. For statistical purposes, each test was repeated three times. All results are presented as the mean of three measurements (n=3), and the error bars in the graphs represent the standard deviation expressed as a percentage of the mean values. To evaluate the mass wear of the graphite samples, they were weighed before and after the friction test. The degree of wear was determined using Equation (1):

$$\text{wear}(\text{wt}\%) = \frac{m_1 - m_2}{m_1} * 100\% \quad (1)$$

where: m_1 — mass of the sample before the friction test, m_2 — mass of the sample after the friction test.

After the completion of the tribological tests, the steel surfaces covered with graphite were examined for morphology using scanning electron microscopy (SEM) and for chemical composition using energy-dispersive X-ray spectroscopy (EDS).

Results of the tests

Analysis of friction indicators and temperature of the tested material pairs

The recorded changes in friction torque over time for selected material pairs operating under dry and water-lubricated conditions are shown in Figure 2. For the EG packing–steel pair, under dry conditions the friction torque remains at approximately 0.87Nm. In the presence of water, this value stabilizes after a few minutes of operation at around 0.4Nm. In the case of the NG packing–steel pair, under dry conditions the friction torque stabilizes after about 10 minutes and reaches a value of approximately 2Nm. In contrast, operation of the same pair in the water environment results in a reduction of friction torque to about 1Nm.

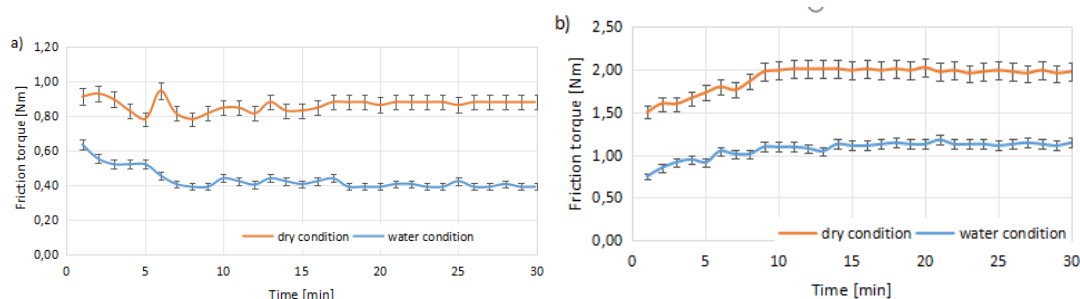


Figure 2. Changes in friction torque over time under dry and water-lubricated conditions for material pairs: (a) EG packing–alloy steel, (b) NG packing–alloy steel

Rysunek 2. Zmiany momentu tarcia w czasie w warunkach suchych i mokrych dla par materiałowych: (a) pakunek EG - stal stopowa, (b) pakunek NG - stal stopowa

The recorded changes in COF for the tested material pairs operating under dry and water-lubricated conditions are shown in Figure 3. Similar trends in COF variation were observed as in the case of friction torque. For the material pair containing expanded graphite, under dry conditions COF remained at approximately 0.11. Operation in the presence of water resulted in a decrease of COF to about 0.06. In the case of the second material pair (with natural graphite), COF under dry conditions was around 0.24, while in the water environment it decreased to about 0.15.

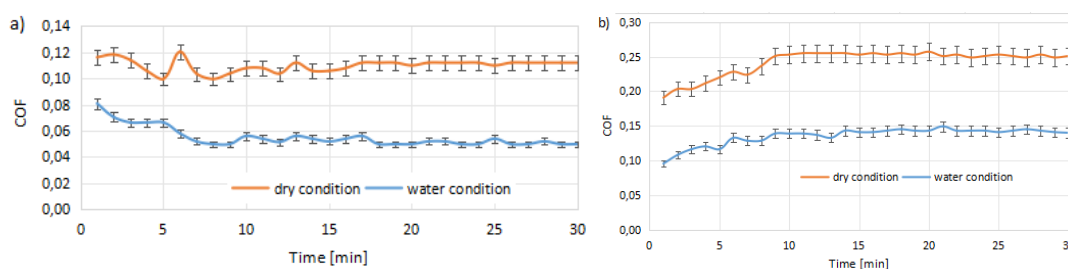


Figure 3. Changes in COF over time under dry and water-lubricated conditions for material pairs: (a) EG packing – alloy steel, (b) NG packing–alloy steel

Rysunek 3. Zmiany COF w czasie, w warunkach suchych i wilgotnych dla par materiałowych: (a) pakunek EG - stal stopowa, (b) pakunek NG - stal stopowa

The average values of friction torque and COF, depending on the operating conditions and the type of material, are shown in Figure 4. Under dry conditions, the use of packing with natural graphite instead of expanded graphite resulted in an increase in friction torque by 120% and COF by 119%. Even greater differences were observed in the presence of water — compared to the sample with expanded graphite, the friction torque for the packing with natural graphite was higher by 149%, while COF increased by 117%.

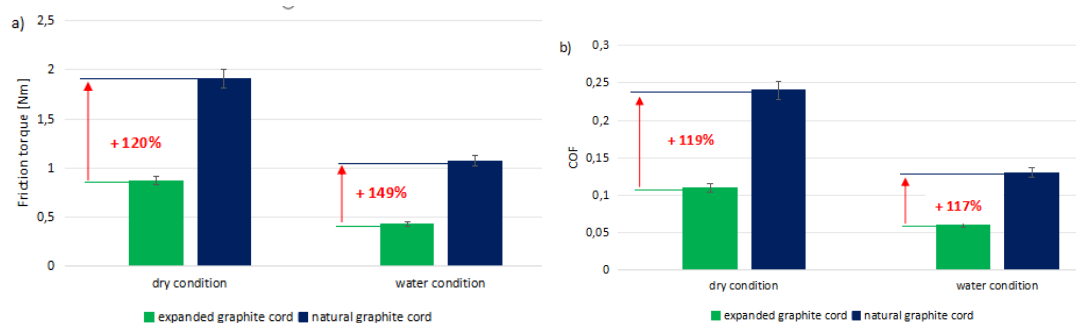


Figure 4. Average values of (a) friction torque and (b) COF for the investigated graphite materials in contact with alloy steel under dry and water-lubricated conditions.

Rysunek 4. Średnie wartości: (a) momentu tarcia oraz (b) COF dla badanych materiałów grafitowych współpracujących ze stalą stopową w warunkach suchych i wodnych

The variations of COF and temperature over time, depending on the type of graphite material applied under dry conditions, are presented in Figure 5. For the pair with natural graphite (dark blue), it was observed that during the first 15 minutes of operation, the COF increased concurrently with the rise in temperature. Beyond this period, the pair attained a steady state, with the temperature stabilizing at approximately 99°C. In contrast, for the pair containing expanded graphite, temperature stabilization occurred considerably faster—after approximately 5 minutes—at a level of about 70°C. The temporal evolution of COF and temperature under water-lubricated conditions is shown in Figure 6. In these conditions, the operating temperatures were markedly lower: approximately 60°C for the pair with natural graphite and 40°C for the pair with expanded graphite. Analogous to the dry regime, temperature stabilization for the natural graphite pair occurred after about 15 minutes, whereas for the expanded graphite pair it was achieved after only 5 minutes. This indicates that the thermal stabilization process in the presence of expanded graphite proceeds approximately three times faster. A plausible explanation for this phenomenon lies in the substantially larger active surface area of expanded graphite, which promotes more effective heat dissipation. The increased active surface—encompassing a greater number of layer edges, pores, and adsorption sites—may also enhance the adsorption of moisture or other species present in the tribological environment, thereby contributing to both the modification and stabilization of the pair's thermal conductivity.

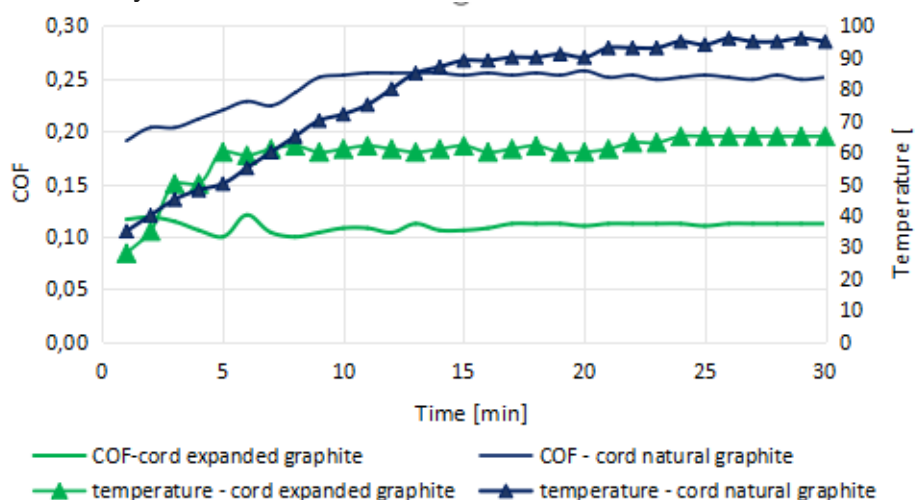


Figure 5. Evolution of COF and temperature over time depending on the type of graphite material under dry conditions

Rysunek 5. Zmiany COF i temperatury w czasie, w zależności od rodzaju materiału grafitowego w suchych warunkach pracy

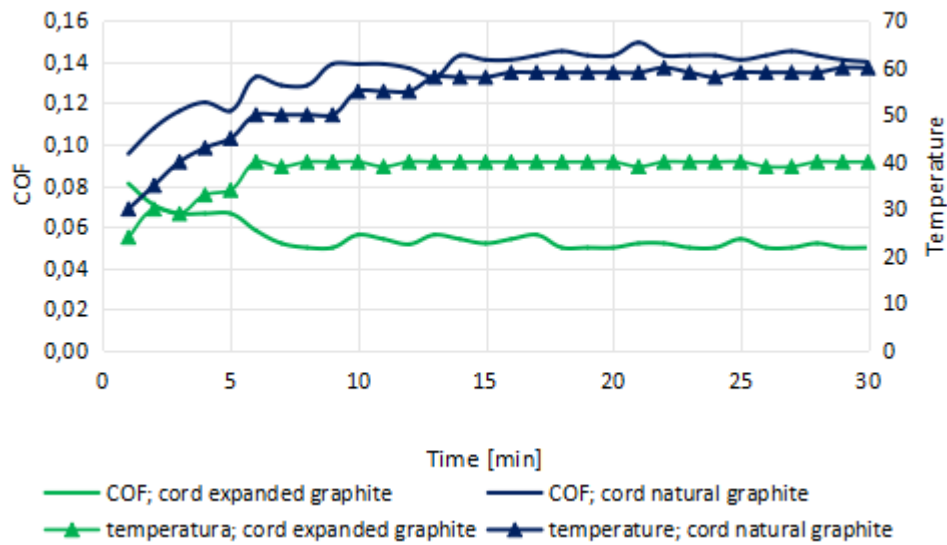


Figure 6. Evolution of COF and temperature over time depending on the type of graphite material under water-lubricated conditions

Rysunek 6. Zmiany COF i temperatury w czasie w zależności od rodzaju materiału grafitowego w środowisku wodnym

The average temperatures of the investigated tribological pairs, depending on the operating conditions and the type of graphite material used, are presented in Figures 7a and 7b. Under dry conditions, the operating temperature of the expanded graphite pair was 32% lower compared to the natural graphite pair. In water-lubricated conditions, this difference increased to 41% in favor of expanded graphite. When analyzing the influence of the operating environment on a given type of graphite, it was observed that the transition from dry to water-lubricated conditions resulted in a temperature decrease of 35% for expanded graphite and 31% for natural graphite.

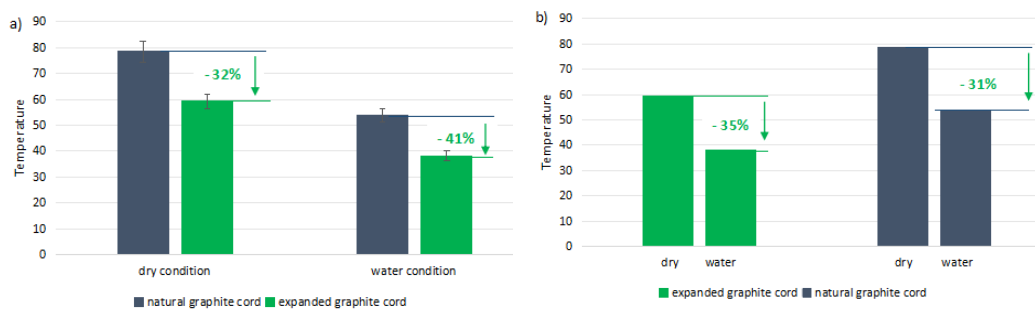


Figure 7. Average temperatures of the investigated tribological pairs as a function of: (a) operating conditions and (b) type of graphite material

Rysunek 7. Średnie temperatury badanych skojarzeń tribologicznych w zależności od: a) warunków pracy, b) rodzaju materiału

Assessment of Mass Wear of Graphite Samples

The analysis of the influence of graphite type and operating conditions on the mass wear of graphite materials is presented in Figures 8a and 8b. Under dry conditions, the use of expanded graphite resulted in a significant reduction in wear—the mass loss was as much as 833% lower compared to the sample with natural graphite. In water-lubricated conditions, this difference was also evident, although less pronounced—the wear of expanded graphite was 129% lower than that of natural graphite. When comparing the effect of the operating environment on a given material, it was observed that expanded graphite loses its resistance properties in the

presence of water — the material wear under water-lubricated conditions increased by as much as 367% relative to dry friction. For natural graphite, this difference was much smaller, amounting to only 15%, which indicates a higher tribological stability of this material under varying environmental conditions. The obtained results demonstrate that, although expanded graphite exhibits considerably higher wear resistance, particularly under dry conditions, its properties may be more sensitive to the presence of water compared to natural graphite, which shows more predictable wear regardless of the operating conditions.

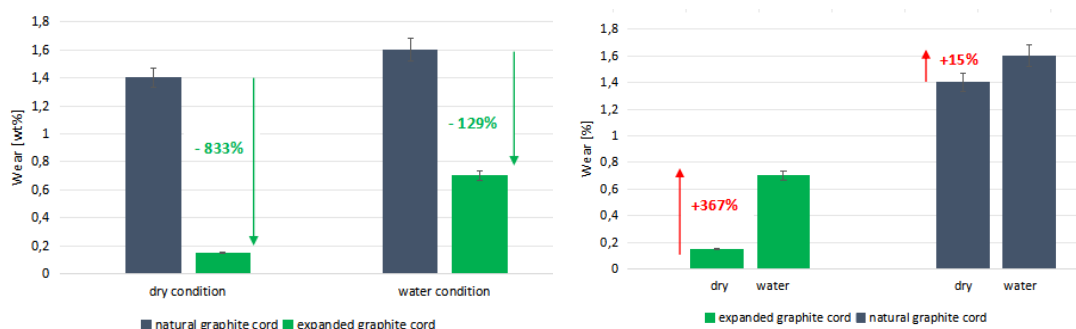


Figure 8. Mass wear of the samples as a function of: (a) operating conditions and (b) type of graphite material
Rysunek 8. Masowe zużycie próbek w zależności od: a) warunków pracy, b) rodzaju materiału

The exceptionally large difference in wear observed under dry conditions can be explained by the combined effects of the anisotropic structure of the materials and the operating temperature of the friction pairs. Expanded graphite (EG), with its more porous and easily deformable layered structure, facilitates the formation of a lubricating layer along the basal planes, allowing smoother sliding and reduced metal-to-metal contact. This effect is enhanced by the thermal behavior of EG: during the tests, EG resulted in a three times faster decrease in the operating temperature of the friction pair, and the average operating temperature was more than 30% lower compared with natural graphite (NG). Lower temperatures reduce thermal degradation of the contact surfaces and help maintain the integrity of the lubricating layer, which, together with the anisotropic sliding mechanism, explains the significantly lower wear observed for EG under dry conditions. The higher wear of NG compared with EG is consistent with the findings of Jin et al. [20], who reported improved tribological performance of EG. Further investigations are necessary to confirm and better understand the mechanisms underlying the observed differences in wear.

Scanning Assessment of Alloy Steel Surface after the Friction Cycle

SEM images of the alloy steel surface after the friction cycle, depending on the operating conditions and the type of graphite material of the samples, are presented in Figure 9. The EDS results are shown in Table 4.

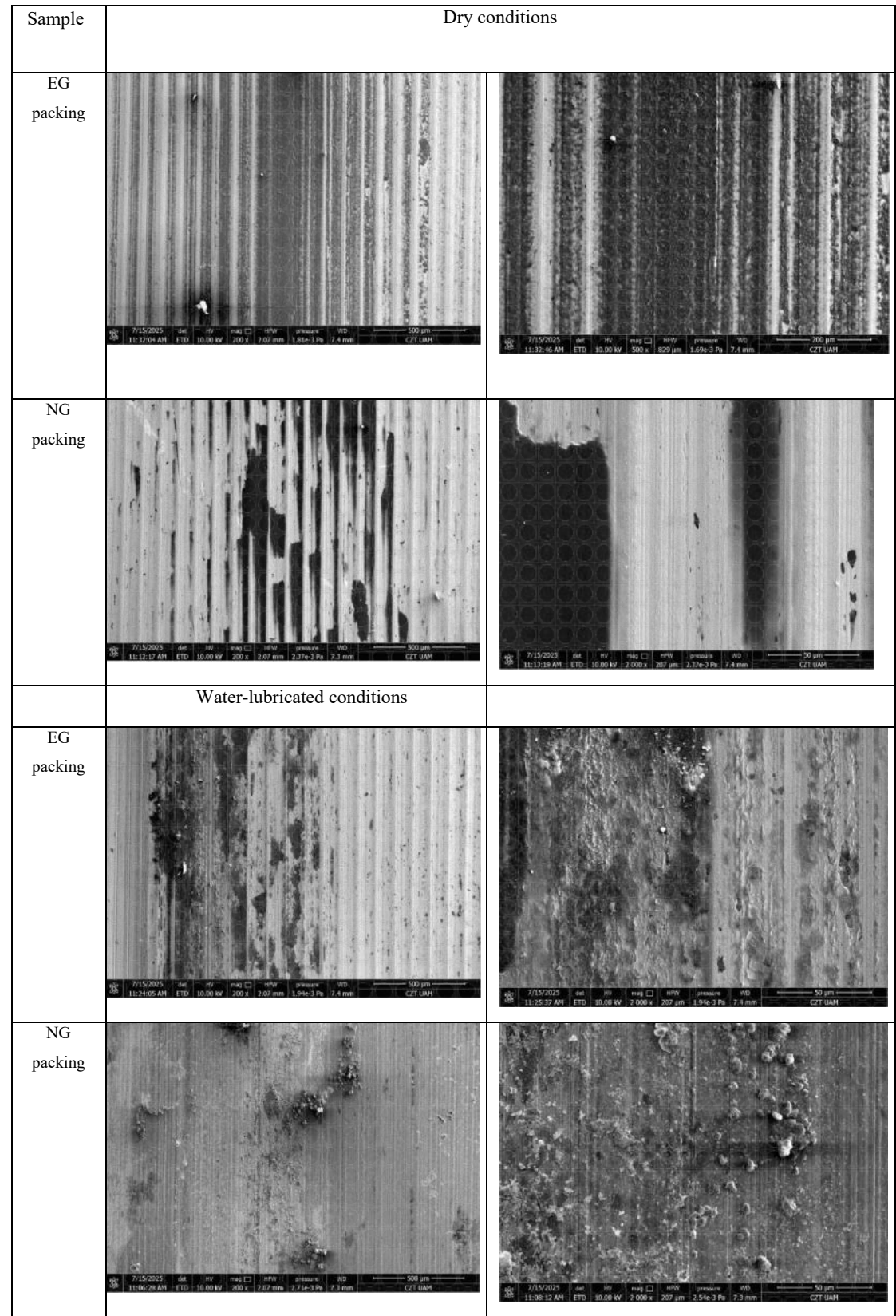


Figure 9. SEM images of the alloy steel surface after the friction cycle depending on operating conditions and the type of graphite material

Rysunek 9. Obrazy SEM powierzchni stali stopowej po cyklu tarcia w zależności od warunków pracy i rodzaju materiału grafitowego

Table 4. EDS results of the alloy steel surface after the friction cycle depending on operating conditions and the type of graphite material

Tabela 4. Wyniki EDS powierzchni stali stopowej po cyklu tarcia w zależności od warunków pracy i rodzaju materiału grafitowego

Sample	Condition	C	Fe	O	Si	S	P	Cr
EG cord	dry	49.72	22.97	11.33	9.63	0.08	0.03	0.24
	water	44.71	31.00	20.34	2.89	0.11	0.06	0.30
NG cord	dry	72.43	19.44	494	0.33	0.10	0.04	0.18
	water	32.43	44.45	1739	0.36	0.44	0.04	0.49

Microscopic observations of the steel surface after the friction cycle revealed distinct differences in the morphology of transfer layers depending on the type of graphite used and the operating conditions. On the surface of steel operating with expanded graphite under dry conditions, a relatively uniformly distributed graphite layer was observed, covering approximately 50% of the analyzed area. The layer filled surface grooves and locally adhered to microasperities, indicating good adhesion and the formation of a continuous tribological film. The characteristics of this layer suggest an adhesive and partially mechanical mechanism, which may indicate effective transfer of material from the packing to the counter-surface. In contrast, the transfer layer formed by natural graphite was characterized by discontinuous coverage—the steel surface coverage reached about 72% by mass, yet the layer was locally irregular. Thicker graphite regions with visible delaminations were observed, which may indicate a greater tendency of this material to fragment or for graphene planes to separate during friction. Such discontinuity of the film may result in a higher COF and more intensive wear.

In the water-lubricated environment, expanded graphite formed a less homogeneous transfer layer (approx. 45% mass coverage), which may be due to partial particle washout or reduced adhesion in the presence of water. The layer exhibited microcracks and delaminations, while graphite also deposited on the tops of asperities. This suggests that the presence of water limits the continuity of the film, but at the same time may provide partial protection of the surface by reducing direct metal-to-metal contact. The least effective transfer layer was formed when natural graphite was applied under water-lubricated conditions. Graphite areas were scarce and distributed in isolated spots (~32% by mass), with limited adhesion to the steel surface. Loosely bound graphite agglomerates, not permanently attached to the substrate, were also present. This suggests a low level of integration of the tribological film in the presence of water and an insufficient self-organization mechanism of the lubricating layer.

Discussion

The obtained results clearly demonstrate that both the operating environment and the type of graphite material used have a significant influence on the course of tribological phenomena in the tested pairs. Distinct differences were observed in COF, friction torque, and sample wear, which were strongly dependent on the type of graphite applied and on whether the operating conditions were dry or water-lubricated.

Under dry conditions, the use of a cord with natural graphite instead of expanded graphite resulted in an increase in COF by 119%, and under water-lubricated conditions by 117%. This indicates clear differences in the operating mechanisms of the two materials and their effectiveness in forming a lubricating layer under different working conditions. The phenomenon of lubricating layer formation is based on the transfer of graphite particles onto the steel surface, which over time may lead to a change in the contact conditions from graphite–steel to graphite–graphite. The transfer mechanism results from mechanical and adhesive interactions arising from the microscopic heterogeneity of frictional surfaces. The conducted tests demonstrated that the nature and intensity of this process depend on both the operating conditions (dry or wet) and the properties of the graphite material.

Chemical composition analysis of the steel surfaces after testing revealed that the carbon content was significantly lower after operation in the water-lubricated environment compared to dry conditions. For the expanded graphite pair, the carbon content decreased by 11%, whereas for the natural graphite pair the difference was much larger, reaching as much as 123%. This indicates that, in the presence of water, graphite transfer to the steel surface was much less effective, particularly for natural graphite, which may have limited the formation of a durable lubricating film. This phenomenon is consistent with the findings of Jia et al. [24] and Hirani and Goilkar [25], who reported that the presence of water can hinder the formation of a graphite layer. Research also indicates that the amount of water supplied to the pair is an important factor affecting frictional mechanisms. According to the results of Tahir et al. [34], the lowest values of friction and wear for graphite coatings were obtained at relative humidities of 55% and 95%. Water molecules adsorbed on the graphite surface act as a lubricant, enabling the sliding of graphite layers relative to each other. However, at 95% humidity, agglomeration of graphite particles occurs, leading to excessive adhesive wear and reduced film durability compared to moderate humidity conditions (55%). High humidity may also result in the binding action of water molecules, which bond graphite particles together and limit their mobility.

The presence of water also reduces friction by lowering adhesive forces and facilitating the movement of graphite layers, which—due to their lamellar structure and weak interlayer bonding—can easily slide relative to one another [35]. Additionally, Bhowmick et al. [36] and Li et al. [37] highlighted the important role of the amorphous carbon structure, which contains numerous edges and dangling bonds that readily react with water molecules. Cyclic degradation and reconstruction of this structure results in COF fluctuations, whereas high moisture levels can passivate these bonds, contributing to a reduction in friction.

At the same time, under water-lubricated conditions, EDS analysis revealed a significant increase in oxygen content on the steel surface—twofold in the case of expanded graphite, and as much as fourfold for natural graphite. These observations are consistent with the findings of Restuccia et al. [26], who demonstrated that the presence of water in a tribological pair promotes the formation of oxides on the metal surface, influencing friction characteristics. Oxygen, originating both from water and from the air, may participate in the passivation of so-called “dangling bonds” at the edges of graphite layers, contributing to friction reduction and stabilization of the lubricating film.

The conducted tests also showed that the presence of water led to increased wear (Fig. 8). The increase in wear under wet conditions may be attributed to intensified adhesion or to the unstable behavior of the graphite layer in the presence of water. For both materials, an increase in wear was observed when transitioning to water-lubricated conditions. Natural graphite exhibited higher mass wear (Fig. 8a), however, analysis revealed that expanded graphite showed a greater relative increase in wear as a result of the change from dry to wet conditions (Fig. 8b). This may indicate a higher sensitivity of expanded graphite’s structure to the presence of water, despite its beneficial effect on friction. Studies by Rewolińska et al. [38] confirm that in the expanded graphite–steel pair, during cyclic water exposure, sharp fluctuations in COF and friction torque were observed, indicating lower stability and predictability of this material’s performance in a water environment, which may be reflected in its wear behavior.

The type of graphite applied also had a significant effect on the operating temperature of the tribological system. In both dry and wet conditions, clearly higher temperature values were recorded for natural graphite. The use of expanded graphite enabled a reduction in the operating temperature of the system by about 30% under dry conditions and by 40% under wet conditions, indicating its more favorable properties in terms of heat dissipation. The results further showed that the expanded graphite–steel pair reached thermal stabilization three times faster compared to the natural graphite pair. This phenomenon can be attributed to the larger active surface area and porosity of expanded graphite, which enable more efficient heat dissipation and enhanced moisture adsorption. Both of these factors promote faster activation of the water–graphite lubrication mechanism, contributing to the stabilization of friction parameters already in the early phase of system operation. The obtained results unequivocally confirm the advantageous

properties of expanded graphite in terms of heat management and stabilization of tribological conditions, both in dry and wet environments.

The results of this study are largely consistent with earlier literature reports on tribological processes in systems involving carbon-based materials. As described by Chen et al. [39], the material transfer mechanism is strongly correlated with operating conditions. Similar relationships regarding the influence of moisture on the tribological properties of metallic materials were reported by Bregliozzi et al. [40] and De Bates et al. [41], who showed that in humid environments the chemical bonding processes of carbon with the metal surface are intensified, leading to reduced friction. However, Jia et al. [24] demonstrated that for a bronze–graphite composite, the presence of water increased COF compared to dry conditions. On the other hand, the wear rate of the composite decreased under wet conditions. This was attributed to the hindered transfer of composite material onto the steel surface during friction in the presence of water. It follows that tribological phenomena associated with the presence of water in systems involving carbon materials have not yet been fully elucidated.

Conclusions

The conducted study enabled a comparison of the tribological properties of braided packings containing natural graphite and expanded graphite under dry and water-lubricated conditions. The obtained results allow the following conclusions to be drawn:

1. Both the type of graphite (natural or expanded) and the operating conditions (dry or water-lubricated) have a significant influence on the course of tribological processes in the tested material pairs.
2. Under both dry and water-lubricated conditions, expanded graphite exhibited significantly better lubricating properties than natural graphite. The COF was lower by 119% in dry conditions and by 117% in water-lubricated conditions.
3. Both materials showed higher mass wear in water-lubricated conditions compared to dry conditions. However, expanded graphite was characterized by a distinctly lower mass loss than natural graphite. Under dry conditions, the mass wear of expanded graphite was as much as 833% lower, while in water-lubricated conditions this difference amounted to 129% in its favor.
4. Expanded graphite promoted more efficient heat dissipation, as evidenced by the lower operating temperature of the system (30–40% lower compared to natural graphite) and three times faster thermal stabilization.
5. SEM and EDS analyses revealed that expanded graphite forms more uniform and adhesive transfer layers under dry conditions, which promotes friction stabilization. In water-lubricated conditions, these layers became less homogeneous. Natural graphite showed weak adhesion to the substrate and discontinuous coverage of the steel surface.

The obtained results confirm that the proper selection of graphite type according to operating conditions is crucial for ensuring the durability and efficiency of tribological components in engineering applications.

References

1. Gbadeyan O.J., Kanny K.: Tribological behaviors of polymer–based hybrid nanocomposite brake pad, *Journal of Tribology*, 140, 2018, 032003.
2. Oshita K., Komiyama S., Sasaki S.: Preparation of a mica–organic hybrid solid lubricant and characterization of its lubrication mechanisms, *Tribology International*, 123, 2018, 349–358.
3. Österle W., Dmitriev A.: The role of solid lubricants for brake friction materials, *Lubricants*, 4, 5, 2016.
4. Kayode J.F., Afolalu S.A., Emeteri M.E., Monye S.I., Sunday L., Lawa S.L.: Application and impact of tribology in energy – an overview, *E3S Web Conference*, 2023, 391, 01081.

5. Cui J., Zhao J., Wang S., Wang Y., Li Y.: Effects of carbon nanotubes functionalization on mechanical and tribological properties of nitrile rubber nanocomposites, *Molecular dynamics simulations, Computational Materials Science*, 196, 2021, 110556.
6. Sengupta R., Bhattacharya M., Bandyopadhyay S., Bhowmick A.K.: A review on the mechanical and electrical properties of graphite and modified graphite reinforced polymer composites, *Journal of Materials Science*, 7, 2002, 1475–1489.
7. Hajdukiewicz G., Komarov A.I., Orda D.V., Panasiuk K.: Analysis of the Impact of Graphite Addition on the Tribological Properties of Composites with Polyester–Glass Recyclate, *Materials*, 18(2), 2025, 376.
8. Baptista R., Mendão A., Rodrigues F., Figueiredo-Pina C.G., Guedes M., Marat-Mendes R.: Effect of high graphite filler contents on the mechanical and tribological failure behavior of epoxy matrix composites, *Theoretical and Applied Fracture Mechanics*, 85, 2016, 113–124.
9. Alajmi M., Alrashdan K.R., Alsaeed T., Shalwan A.: Tribological characteristics of graphite epoxy composites using adhesive wear experiments, *Journal of Materials Research and Technology*, 9, 6, 2020, 13671–13681.
10. Kolluri D.K., Boidin X., Desplanques Y., Degallaix G., Ghosh A.K., Kumar M., Bijwe J.: Effect of natural graphite particle size in friction materials on thermal localisation phenomenon during stop–braking, *Wear*, 268, 2010, 1472–1482.
11. Kolluri D.K., Satapathy B.K., Bijwe J., Ghosh A.K.: Analysis of load and temperature dependence of tribo–performance of graphite filled phenolic composites, *Materials Science and Engineering: A, Structural Materials: Properties, Microstructure and Processing*, 456, 2007, 162–169.
12. Aranganathan N., Bijwe J.: Comparative performance evaluation of NAO friction materials containing natural graphite and thermo-graphite, *Wear*, 358–359, 2016, 17–22.
13. Demi M.E., The effect of graphite addition on the friction coefficient and wear behavior of glass fiber reinforced composites, *Uludağ University Journal of The Faculty of Engineering*, 29(1), 2024, 113–124.
14. Basavarajappa S., Ellangovan S.: Dry sliding wear characteristics of glass–epoxy composite filled with silicon carbide and graphite particles, *Wear*, 296(1–2), 2012, 491–496.
15. Basavarajappa S., Ellangovan S., Arun, K.V.: Studies on dry sliding wear behaviour of graphite filled glass–epoxy composite, *Materials & Design*, 30(7), 2009, 2670–2675.
16. Dinker A., Agarwal M., Agarwal G.D.: Preparation, characterization, and performance study of beeswax/expanded graphite composite as thermal storage material, *Experimental Heat Transfer*, 30, 2017, 139–150.
17. Struchkova T.S., Okhlopko A.A., Sleptsova S.A.: Triboengineering properties of polytetrafluoroethylene modified by thermally expanded graphite, *Journal of Friction and Wear*, 29, 2008, 381–385.
18. Wang L.L., Zhang L.Q., Tian M.: Effect of expanded graphite (EG) dispersion on the mechanical and tribological properties of nitrile rubber/EG composites, *Wear*, 276–277, 2012, 85–93.
19. Jia Z.N., Hao C.Z., Yan Y.H., Yang Y.L.: Effects of nanoscale expanded graphite on the wear and frictional behaviors of polyimide–based composites, *Wear*, 338–339, 2015, 282–287.
20. Jin H., Zhou K., Ji Z. et al.: Comparative tribological behavior of friction composites containing natural graphite and expanded graphite, *Friction* 8, 2020, 684–694.
21. Morstein C.E., Klemen A., Dienwiebel M., Moseler M.: Humidity-dependent lubrication of highly loaded contacts by graphite and a structural transition to turbostratic carbon, *Nature Communications*, 13(1), 2022, 5958.
22. Hasz K., Ye Z., Martini A., Carpick R.W.: Experiments and simulations of the humidity dependence of friction between nanoasperities and graphite: The role of interfacial contact quality, *Physical Review Materials*, 2(12), 2018, 126001.

23. Plaza S., Margielewski L., Celichowski G.: Introduction to Tribology and Tribochemistry, WUŁ, Łódź, Poland, 2005.
24. Jia J.H., Chen J.M., Zhou H.D., Wang J.B., Zhou H.: Friction and wear properties of bronze-graphite composite under water lubrication, *Tribology International*, 2004, 37, 423–429.
25. Hirani H., Goilkar, S.S.: Formation of transfer layer and its effect on friction and wear of carbon-graphite face seal under dry, water and steam environments, *Wear*, 2009, 266, 1141–1154.
26. Restuccia P., Ferrario M., Righi M.C.: Monitoring water and oxygen splitting at graphene edges and folds: Insights into the lubricity of graphitic materials, *Carbon*, 156, 2020, 93–103.
27. Borruto A., Crivellone G., Marani F.: Influence of surface wettability on friction and wear tests, *Wear*, 222, 1998, 57–65.
28. Jia J.H., Chen J.M., Zhou H.D., Hu L.T., Chen L.: Comparative investigation on the wear and transfer behaviors of carbon fiber reinforced polymer composites under dry sliding and water lubrication, *Composites Science and Technology*, 65, 2005, 1139–1147.
29. Lancaster J.K.: A review of the influence of environmental humidity and water on friction, lubrication and wear, *Tribology International*, 23(6), 1990, 371–389.
30. Lancaster J.K.: Lubrication of carbon fiber-reinforced polymers. Part I: Water and aqueous solutions, *Wear*, 203, 1972, 15–330.
31. Moosa A.A., Mayyadah S.A.: Graphene preparation and graphite exfoliation, *Turkish Journal of Chemistry*, 45(3), 2021, 493–519.
32. Asenbauer J., Eisenmann T., Kuenzel M., Kazzazi A., Chen Z., Bresser D.: The success story of graphite as a lithium-ion anode material – fundamentals, remaining challenges, and recent developments including silicon (oxide) composites, *Sustainable Energy Fuels*, 4, 2020, 5387–5416.
33. Coetzee D., Perez Aguilera J.P., Šubrova T., Wiener J., Militký J.: Expanded graphite to enhance the conductive and mechanical properties of geopolymer PVA and epoxy, Conference materials NANOCON, 2023.
34. Tahir N.A.M., Liza S., Fukuda K., Yaakob Y., Zulkifli N.A., Rawian N.A.M., Ghazazi N.A.M.: Influence of humidity on the tribological performance of graphite reinforced aluminium anodic oxide coating, *Tribology International*, 197, 2024, 109752.
35. Scharf T., Prasad S.: Solid lubricants: A review, *Journal of Materials Science*, 48, 2012, 511–531.
36. Bhowmick S., Banerji A., Alpas A.T.: Role of humidity in reducing sliding friction of multilayered graphene, *Carbon*, 87, 2015, 374–384.
37. Li Z., Yang W., Wu Y., Wu S., Cai Z.: Role of humidity in reducing the friction of graphene layers on textured surfaces, *Applied Surface Science*, 403, 2017, 362–370.
38. Rewolińska A., Leksycki K., Wojciechowski Ł., Perz K.: Analysis of Tribological Properties of Expanded Graphite—Alloy Steel Pair Under High Loads in Dry and Humid Conditions, *Applied Sciences*, 15(7), 2025, 4022.
39. Chen Z., He X., Xiao C., Kim S.H.: Effect of Humidity on Friction and Wear—A Critical Review, *Lubricants*, 6, 2018, 74.
40. Bregliozzi G., Di Schino A., Kenny J.M., Haefke H.: The influence of atmospheric humidity and grain size on the friction and wear of AISI 304 austenitic stainless steel, *Materials Letters*, 57, 2003, 4505–4508.
41. De Baets P., Kalacska G., Strijckmans K., Van de Velde F., Van Peteghem A.P.: Experimental study by means of thin layer activation of the humidity influence on the fretting wear of steel surfaces, *Wear*, 216, 1998, 131–137.